Measurement of the Inclusive B^* Cross Section above the $\Upsilon(4S)$

D. S. Akerib,[1] B. Barish,[1] D. F. Cowen,[1] G. Eigen,[1] R. Stroynowski,[1] J. Urheim,[1] A. J. Weinstein,[1] R. J. Morrison,[2] D. Schmidt,[2] M. Procario,[3] D. R. Johnson,[4] K. Lingel,[4] P. Rankin,[4] J. G. Smith,[4] J. Alexander,[5] C. Bebek,[5] K. Berkelman,[5] D. Besson,[5] T. E. Browder,[5] D. G. Cassel,[5] E. Cheu,[5] D. M. Coffman,[5] P. S. Drell,[5] R. Ehrlich,[5] R. S. Galik,[5] M. Garcia-Sciveres,[5] B. Geiser,[5] B. Gittelman,[5] S. W. Gray,[5] D. L. Hartill,[5] B. K. Heltsley,[5] K. Honscheid,[5] J. Kandaswamy,[5] N. Katayama,[5] D. L. Kreinick,[5] J. D. Lewis,[5] G. S. Ludwig,[5] J. Masui,[5] J. Mevissen,[5] N. B. Mistry,[5] S. Nandi,[5] C. R. Ng,[5] E. Nordberg,[5] C. O'Grady,[5] J. R. Patterson,[5] D. Peterson,[5] M. Pisharody,[5] D. Riley,[5] M. Sapper,[5] M. Selen,[5] H. Worden,[5] M. Worris,[5] P. Avery,[6] A. Freyberger,[6] J. Rodriquez,[6] J. Yelton,[6] K. Kinoshita,[7] F. Pipkin,[7] R. Wilson,[7] J. Wolinski,[7] D. Xiao,[7] A. J. Sadoff,[8] R. Ammar,[9] P. Baringer,[9] D. Coppage,[9] R. Davis,[9] P. Haas,[9] M. Kelly,[9] N. Kwak,[9] H. Lam,[9] S. Ro,[9] Y. Kubota,[10] J. K. Nelson,[10] D. Perticone,[10] R. Poling,[10] S. Schrenk,[10] M. S. Alam,[11] I. J. Kim,[11] B. Nemati,[11] V. Romero,[11] C. R. Sun,[11] P.-N. Wang,[11] M. M. Zoeller,[11] G. Crawford,[12] R. Fulton,[12] K. K. Gan,[12] T. Jensen,[12] H. Kagan,[12] R. Kass,[12] R. Malchow,[12] F. Morrow,[12] J. Whitmore,[12] P. Wilson,[12] F. Butler,[13] X. Fu,[13] G. Kalbfleisch,[13] M. Lambrecht,[13] P. Skubic,[13] J. Snow,[13] P.-L. Wang,[13] D. Bortoletto,[14] D. N. Brown,[14] J. Dominick,[14] R. L. McIlwain,[14] D. H. Miller,[14] M. Modesitt,[14] E. I. Shibata,[14] S. F. Schaffner,[14] I. P. J. Shipsey,[14] M. Battle,[15] H. Kroha,[15] K. Sparks,[15] E. H. Thorndike,[15] C.-H. Wang,[15] M. Artuso,[16] M. Goldberg,[16] T. Haupt,[16] N. Horwitz,[16] V. Jain,[16] R. Kennett,[16] G. C. Moneti,[16] Y. Rozen,[16] P. Rubin,[16] T. Skwarnicki,[16] S. Stone,[16] M. Thusalidas,[16] W.-M. Yao,[16] G. Zhu,[16] A. V. Barnes,[17] J. Bartelt,[17] S. E. Csorna,[17] T. Letson,[17] and M. D. Mestayer[17]

(CLEO II Collaboration)

[1]*California Institute of Technology, Pasadena, California 91125*
[2]*University of California at Santa Barbara, Santa Barbara, California 93106*
[3]*Carnegie-Mellon University, Pittsburgh, Pennsylvania, 15213*
[4]*University of Colorado, Boulder, Colorado 80309-0390*
[5]*Cornell University, Ithaca, New York 14853*
[6]*University of Florida, Gainesville, Florida 32611*
[7]*Harvard University, Cambridge, Massachusetts 02138*
[8]*Ithaca College, Ithaca, New York 14850*
[9]*University of Kansas, Lawrence, Kansas 66045*
[10]*University of Minnesota, Minneapolis, Minnesota 55455*
[11]*State University of New York at Albany, Albany, New York 12222*
[12]*Ohio State University, Columbus, Ohio 43210*
[13]*University of Oklahoma, Norman, Oklahoma 73019*
[14]*Purdue University, West Lafayette, Indiana 47907*
[15]*University of Rochester, Rochester, New York 14627*
[16]*Syracuse University, Syracuse, New York 13244*
[17]*Vanderbilt University, Nashville, Tennessee 37235*

(Received 20 May 1991)

Using the CLEO II detector at the Cornell Electron Storage Ring, we have determined the inclusive B^* cross section above the $\Upsilon(4S)$ resonance in the energy range from 10.61 to 10.70 GeV. We also report a new measurement of the energy of the $B^* \to B\gamma$ transition photon of $46.2 \pm 0.3 \pm 0.8$ MeV.

PACS numbers: 13.65.+i, 11.30.Er, 13.40.Hq, 14.40.Jz

We report a measurement of the inclusive B^* cross section as a function of center-of-mass energy just above the $\Upsilon(4S)$ resonance. The value of the $B\bar{B}^*$ [1] cross section is necessary to determine the feasibility of observing time-integrated CP-violating asymmetries at a symmetric B factory [2]. We can also compare the hadronic cross section in this energy region with predictions of several potential models [3]. The inclusive B^* cross section is determined by measuring the yield of photons from the transition $B^* \to B\gamma$. The branching fraction for this transition is 100% because the mass difference between the B^* and the B mesons is too small to allow for the emission of a pion.

The data used in this analysis consist of 57.8 pb^{-1}

recorded at five center-of-mass energies between 10.61 and 10.65 GeV, which are above $B\bar{B}^*$ threshold but below $B^*\bar{B}^*$ threshold, and 5.7 pb^{-1} recorded at 10.70 GeV, which is above $B^*\bar{B}^*$ threshold. The energy and integrated luminosity for each point in the scan are given in Table I. We also use 31.3 pb^{-1} collected on the $\Upsilon(4S)$ resonance and 32.3 pb^{-1} taken at energies just below $B\bar{B}$ threshold, and referred to hereafter as the continuum sample. The data were recorded using the new CLEO II detector at the Cornell Electron Storage Ring (CESR). CLEO II is a large solenoidal magnet spectrometer and calorimeter [4]. Tracking is accomplished with a 6-layer straw tube detector, a 10-layer vertex drift chamber [5], and a 51-layer drift chamber system [6] in a 1.5-T magnetic field. Inside the superconducting magnet coil is a calorimeter consisting of a system of 7800 CsI crystals that achieves an rms energy resolution of 1.5% at 5 GeV, 4.1% at 100 MeV [7], and 6.0% at 50 MeV.

The first step of the analysis is the hadronic-event selection. Events that have fewer than five reconstructed charged tracks are discarded. The total visible energy of the event must be greater than $0.4E_{\rm c.m.}$, where $E_{\rm c.m.}$ is the center-of-mass energy. In addition, there must be more than 2 GeV of energy measured by the crystal calorimeter. To reduce backgrounds from beam-wall and beam-gas interactions, we demand that $E_\perp$ be greater than $0.4E_{\rm c.m.}$, where $E_\perp=\sum_i E_i\sin\theta_i$. E_i is the energy of each particle, neutral or charged, with charged particles assumed to be pions. θ_i is the angle between the particle and the beam axis. We reject events with large energy asymmetry by requiring that the ratio $R_1=H_1/H_0$ be less than 0.4, where H_i is the ith Fox-Wolfram moment [8] determined from both charged tracks and photon candidates. In addition, we require that events be spherical in shape by demanding $R_2\leq 0.15$, where $R_2=H_2/H_0$. This cut on event shape effectively removes continuum events which are jetlike and preserves $B\bar{B}$ events which are more spherical. The efficiency for the hadronic selection requirements described above is determined by comparing the number of continuum-subtracted $\Upsilon(4S)$ events passing these cuts with the measured $\Upsilon(4S)$ cross section [9] of 1150 pb. The total hadronic-event-selection efficiency for $B\bar{B}$-like $\Upsilon(4S)$ decays passing the cut $R_2\leq 0.15$ is $(55.4\pm 0.6)\%$, where the error on the efficiency is statistical.

Table I. Summary of results.

$E_{\rm c.m.}$ (GeV)	L (pb^{-1})	$\sigma_{b\bar{b}}$ (pb)	σ_{B^*} (pb)
10.58	31.3	1150	$-15\pm 15\pm 10$
10.61	9.7	$215\pm 13\pm 46$	$58\pm 18\pm 17$
10.62	12.9	$243\pm 12\pm 9$	$151\pm 20\pm 30$
10.63	9.8	$243\pm 12\pm 15$	$164\pm 23\pm 22$
10.64	9.7	$218\pm 13\pm 18$	$121\pm 21\pm 21$
10.65	15.8	$156\pm 11\pm 21$	$151\pm 18\pm 17$
10.70	5.7	$226\pm 17\pm 28$	$346\pm 34\pm 46$

Candidate photons in the hadronic-event sample are found as clusters in the CsI calorimeter. Cuts are made on the cluster shape to distinguish isolated electromagnetic showers, which have a narrow lateral spread, from nonelectromagnetic showers. Photon candidates are required to lie in the best region of the barrel calorimeter, $|\cos\theta|<0.71$; photon candidates are not allowed to match the projection of any charged track. The photon finding efficiency is determined by generating $B^*\rightarrow B\gamma$ decays with the correct angular distributions in a Monte Carlo simulation and then embedding the photon from the $B^*\rightarrow B\gamma$ decay in real events that have passed the hadronic-event-selection requirements. In the hadronic-event sample, the efficiency for finding 50-MeV photons from $B^*\rightarrow B\gamma$ decays, including the solid angle requirement, is $(50.4\pm 1.2)\%$.

We perform an alternative analysis using hadronic events tagged with a high-momentum lepton. The lepton-tagging requirement significantly enhances the fractional b-quark content of the sample by rejecting continuum events. For events with an identified lepton the requirement on R_2 is loosened to $R_2\leq 0.25$. With the looser shape cut, the event-selection efficiency is $(75.7\pm 0.8)\%$. We analyze the data using both methods, exclude the lepton-tagged events from the inclusive sample, and form the weighted average of the results from the two samples to obtain the final result.

Candidate electrons are selected on the basis of tracking and shower information. Each electron candidate is required to have a momentum greater than 1.0 GeV/c and match a shower located in the barrel of the crystal calorimeter. To identify electrons, we combine information from the dE/dx measurements in the central drift chamber with the ratio of the energy measured in the calorimeter to the momentum determined from the tracking system. In order to select muons we require hits in the muon system that match the extrapolated position of a charged track. The selection criteria remove most muons with momenta of less than 1.4 GeV/c.

The effective efficiency for tagging B decays with leptons is determined from continuum-subtracted $\Upsilon(4S)$ data. The events have to pass the hadronic-event selection and the lepton-tagging requirements. The effective efficiency for tagging a B decay with a muon or electron (including the momentum cut, the momentum spectrum of leptons from B decay, and the branching fractions to electrons and muons) is $(15.5\pm 0.3)\%$.

In order to determine the $B\bar{B}^*$-production cross section as a function of energy, we simultaneously fit the continuum-subtracted photon energy spectrum at each of the energy scan points below $B^*\bar{B}^*$ threshold. (The simultaneous fit includes both the inclusive spectra and the lepton-tagged spectra.) The continuum photon spectrum is scaled by the ratio of luminosities and by the inverse ratio of energies squared, and then subtracted bin by bin from the photon energy spectrum at each scan energy. This removes approximately 60% of the background from

the inclusive photon spectrum and the background that remains is well modeled with a second-order polynomial, whose parameters are allowed to vary from one scan energy to the next. The B^* photon line is described by a Doppler-broadened line shape which is smeared with a Gaussian detector resolution. The contribution of the detector resolution to the width of the photon line is a single free parameter in the fit, but is constrained to lie between 2.7 and 3.3 MeV [10]. The Doppler broadening depends on the center-of-mass energy, but involves no other free parameters. The mean energy of the $B^* \to B\gamma$ photon is constrained to be the same for each of the scan points. From the global fit, we find that the mean photon energy is $46.2 \pm 0.3 \pm 0.8$ MeV. The systematic error is the sum of quadrature of two components, one from the uncertainty in background shape (0.7 MeV) and a second due to the uncertainty in the absolute photon energy scale (0.35 MeV). The latter is determined from studies of the decays $\pi^0 \to \gamma\gamma$ and $\Sigma^0 \to \Lambda\gamma$. Figure 1 shows the result of the fit to one of the inclusive photon spectra. For the scan energy above the $B^*\bar{B}^*$ threshold, we fit the continuum-subtracted photon spectrum to a second-order polynomial and a Gaussian line shape. We do not constrain the width of the Gaussian, since the relative fractions of $B^*\bar{B}^*$ and $B\bar{B}^*$ events in the sample are not known. We extract the inclusive photon cross section at this energy by counting the number of $B^* \to B\gamma$ transitions.

The cross section for inclusive B^* production is $\sigma_{B^*} = N_\gamma/(\epsilon \int \mathcal{L}\, dt)$, where N_γ is the number of observed photons and ϵ is the total detection efficiency. ϵ is the product of the hadronic-selection efficiency, the photon-detection efficiency, and in the case of the lepton-tagged analysis, the effective lepton-tagging efficiency. By normalizing the hadronic-selection efficiencies to the measured $\Upsilon(4S)$ cross section, the result for σ_{B^*} depends only on the relative luminosity calibration.

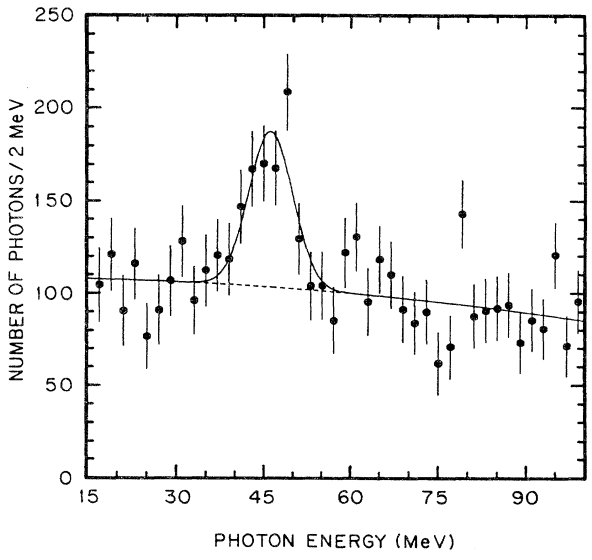

FIG. 1. Fit to the continuum-subtracted inclusive photon spectra for $E_{\text{c.m.}} = 10.63$ GeV.

The largest sources of systematic uncertainty in this measurement are the uncertainty in the photon energy resolution at 46 MeV, and the uncertainty in the shape of the background. In order to estimate the error that results from the uncertainty in the background shape, the data are fitted by the following alternative methods: (a) The background under the photon line is constrained to a combination of continuum plus $\Upsilon(4S)$ in a ratio fixed by the relative luminosities and cross sections, and (b) the background is fitted separately for each of the incident energies by a smooth polynomial without performing a continuum subtraction.

We use the variation in the results from these different methods to estimate the systematic error due to the fitting procedure. To estimate the systematic uncertainty due to the choice of cuts, which is another measure of the uncertainty in the background, we fit the photon spectrum by the three procedures described above and modify the hadronic-event selection by varying the R_2 cut. To estimate the systematic error from the uncertainty in the photon resolution, we vary the Gaussian detector resolution throughout the allowed range for all the fitting procedures. Other sources of systematic error are the photon-finding efficiency (5%), the lepton-finding efficiency (5%), and the relative luminosity calibration (3%). These sources of systematic error are combined in quadrature to arrive at the final systematic error.

The final results, where the first error is statistical and the second is systematic, are given in Table I. We have combined the results from the inclusive and lepton-tagged analyses by excluding the events with leptons from our inclusive sample.

We also determine the total hadronic cross section in excess of the continuum by counting the events that have passed our hadronic-event selection criteria at each energy scan point. We use the relation

$$\sigma_{b\bar{b}} = (1.15\ \text{nb}) \frac{N_* - N_c (L_*/L_c)(E_c^2/E_*^2)}{N_4 - N_c (L_4/L_c)(E_c^2/E_4^2)} \frac{L_4}{L_*},$$

where N_*, N_4, and N_c refer to the number of hadronic events at the scan energy, $\Upsilon(4S)$, and continuum, respectively. $L = \int \mathcal{L}\, dt$ refers to the integrated luminosity and E refers to the beam energy. The above expression takes into account the energy dependence of the continuum cross section. Table I gives the hadronic cross section ($\sigma_{b\bar{b}}$) above the continuum measured at each scan energy. The cross sections measured in the lepton-tagged analysis are in good agreement with those determined from hadronic events if it is assumed that the observed leptons are produced with a rate equal to the B-meson semileptonic decay rate. This indicates that the hadronic cross section above continuum is predominantly $B\bar{B}$-like.

At the scan point above the $B^*\bar{B}^*$ threshold, the measured inclusive B^* cross section exceeds the hadronic

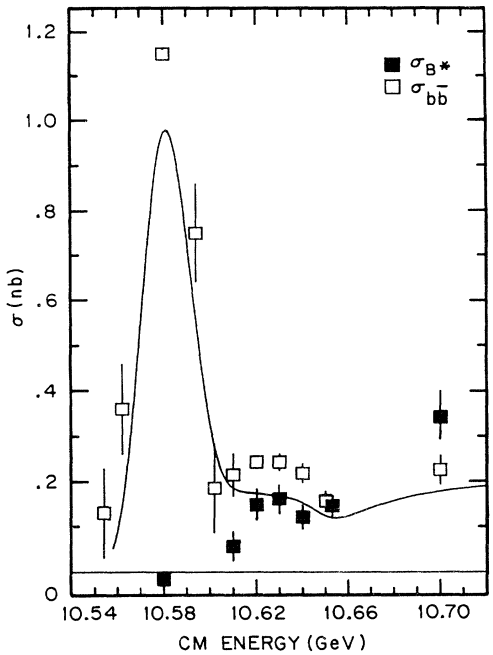

FIG. 2. The cross section for inclusive B^* production as a function of c.m. energy (solid squares) and the hadronic cross section above continuum (open squares). The curve is the prediction for the total hadronic cross section [11] from the Byers and Eichten model in Ref. [3]. This model underestimates the hadronic cross section in the B^* threshold region.

cross section. We conclude that there is significant $B^*\bar{B}^*$ production at this energy point. Figure 2 shows the inclusive B^* cross section as a function of c.m. energy, as well as the hadronic cross section above continuum $q\bar{q}$ production in this energy region. Also shown in Fig. 2 is a prediction for the total hadronic cross section from the potential model calculation of Byers and Eichten [3,11]. The other models in Ref. [3] show a qualitatively similar level of agreement with the data.

In conclusion, we have measured the inclusive B^* cross section as a function of energy in the region just above the $\Upsilon(4S)$. The highest measured value of the $B\bar{B}^*$ cross section below the $B^*\bar{B}^*$ threshold is $164 \pm 23 \pm 22$ pb. This value can be used to estimate the luminosity required [12] to observe CP violation at a symmetric B factory. We have also measured the energy of the photon in the $B^* \rightarrow B\gamma$ transition to be $46.2 \pm 0.3 \pm 0.8$ MeV. This agrees well with the CUSB measurement [13] of 45.4 $\pm$ 1.0 MeV and is consistent with expectations based on scaling mass differences of vector and pseudoscalar mesons [14].

We are grateful for the dedicated efforts of the CESR staff which made this work possible. P.S.D. thanks the Presidential Young Investigator program of the NSF, G.E. thanks the Heisenberg Foundation, K.H. thanks the A. von Humboldt Foundation, and R.P. and P. Rankin thank the A. P. Sloan Foundation for support. This work was supported by the National Science Foundation and the U.S. Department of Energy under Contracts No. DE-AC02(76ER01428, 83ER40103, 76ER03064, 76ER-01545, 78ER05001), and No. DE-FG05-86ER40272.

[1] Throughout this paper, reference to a particle or decay implies the use of its charge conjugate as well. For all the measurements described herein, we sum over the charged and neutral species of B^* and B mesons.

[2] *Proceedings of the Summer Study on High Energy Physics in the 1990's, Snowmass, 1988,* edited by Sharon Jensen (World Scientific, Singapore, 1989).

[3] N. A. Törnqvist, Phys. Rev. Lett. **53**, 878 (1984); S. Ono *et al.*, Phys. Rev. Lett. **55**, 2938 (1985); A. D. Martin and C. K. Ng, Z. Phys. C **40**, 133 (1988); N. Byers and E. Eichten, Nucl. Phys. Proc. Suppl. **B16**, 281 (1990).

[4] E. Blucher *et al.*, Nucl. Instrum. Methods Phys. Res., Sect. A **249**, 201 (1986); C. Bebek *et al.*, Nucl. Instrum. Methods Phys. Res., Sect. A **265**, 258 (1988). Also see E. Cheu, Ph.D. thesis, Cornell University Report No. 91/06 (unpublished); P. Wilson, Ph.D. thesis, Ohio State University, 1991 (unpublished).

[5] C. Bebek *et al.*, Phys. Rev. D **36**, 690 (1987).

[6] D. G. Cassel *et al.*, Nucl. Instrum. Methods Phys. Res., Sect. A **252**, 325 (1986).

[7] T. Skwarnicki, in Proceedings of the Twenty-Fifth International Conference on High Energy Physics (World Scientific, Singapore, to be published).

[8] G. Fox and S. Wolfram, Phys. Rev. Lett. **41**, 1581 (1978).

[9] D. Besson *et al.*, Phys. Rev. Lett. **54**, 381 (1985).

[10] The shape of the final photon distribution is well approximated by a Gaussian line shape. The constraint on the contribution of the detector resolution to width of the photon line was determined from studies of π^0's, $\Upsilon(3S)$ transitions, and Monte Carlo simulations of single photons.

[11] Corrections for initial-state radiation and beam energy smearing have been applied to this model, which has been updated to include the most recent measurements of the B^*- and B-meson masses.

[12] The ratio of the luminosity required to observe CP violation at a symmetric B factory to the luminosity required at an asymmetric B factory is referred to as the luminosity penalty. The value of the luminosity penalty depends on $\sigma(B\bar{B}^*)$, the relative detection efficiencies, and the vertex resolution achieved at an asymmetric B factory. If the CP-violation decay mode is $B^0 \rightarrow \psi K_s$ and lepton tagging is employed to determine the flavor of the opposite B, the luminosity penalty is 7.1 for $\sigma(B\bar{B}^*) = 0.164$ nb. This conclusion assumes equal detection efficiencies for both types of machines. Similar conclusions are derived in Ref. [2].

[13] K. Han *et al.*, Phys. Rev. Lett. **55**, 36 (1985); J. Lee-Franzini *et al.*, Phys. Rev. Lett. **65**, 2947 (1990).

[14] E. Eichten *et al.*, Phys. Rev. D **21**, 203 (1980); S. Godfrey and N. Isgur, Phys. Rev. D **32**, 189 (1985). A small correction of $\sim$0.2 MeV must be applied to convert the energy of B^* transition photon into the mass difference between the B^* and B mesons.